The Penetrability of the Magnetopause Tested by Numerical Integration of Single Particle Orbits

Marius M. Echim

Institute for Space Sciences, Bucharest, Romania

Abstract

The plasma flow in the magnetosheath is non-uniform. Plasma irregularities (or plasmoids) having an excess of momentum with respect to the background can penetrate impulsively through the surface of total (dynamic + kinetic + magnetic) pressure equilibrium - the magnetopause. The polarization electric field distribution can be derived by the first order (guiding center) approximation of the plasma kinetic theory. This E-field distribution is tested by numerical integration of single particle orbits. A $1D$ model of a tangential discontinuity simulates the magnetopause of a "closed" magnetosphere. The results show that particle transport across the magnetic barrier is enabled by the polarization electric field and that the penetration distance depends on the initial total energy of the particle but not on the angle of shear of the magnetic field vector. Finite Larmor radius effects are also illustrated and discussed.

Mechanisms/models

- **magnetic reconnection**: steady-state, large scale (*Dungey*, 1961; *Vasyliunas*, 1976, *Sonnerup*, 1981), cusp reconnection (*Cowley*, 1981; *Song and Russell*, 1992), time-dependent (*Pudovkin and Semenov*, 1985, *Kiendl et al.*, 1992)
- **Kelvin-Helmholtz** instability at the magnetopause (*Dungey*, 1955; *Southwood*, 1968; *Fujimoto and Terasawa*, 1991)

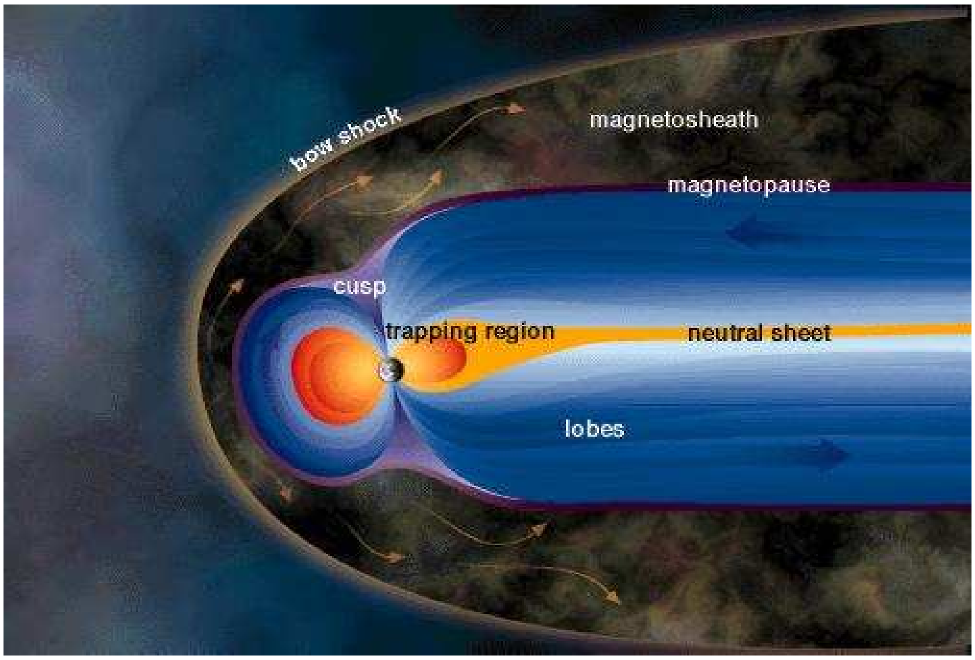

- **diffusion**(*Tsurutani and Thorne*, 1982; *Winske and Omidi*, 1995)
- **pressure pulses** (*Sibeck et al.*, 1989, 1990; *Lin et al.*, 1996)
- **impulsive penetration** (*Lemaire*, 1976, 1985; *Heikkila*, 1982; *Woch and Lundin*, 1992)

Numerical integration of single particle orbits

Equations to integrate:

$$
\begin{aligned}
\frac{d^2\boldsymbol{r}}{dt^2} &= \frac{q}{m}\left[\boldsymbol{E}(\boldsymbol{r}) + \frac{d\boldsymbol{r}}{dt}\times\boldsymbol{B}(\boldsymbol{r})\right] \\
\frac{d\boldsymbol{r_{gc,\perp}}}{dt} &= \boldsymbol{v}_{gc,\perp} \\
\frac{d^2\boldsymbol{r_{gc,\parallel}}}{dt^2} &= \frac{d\boldsymbol{v}_{gc,\parallel}}{dt}
\end{aligned}
\qquad (1)
$$

where:

$$
\begin{aligned}
\boldsymbol{v}_{gc,\perp} &= \frac{\boldsymbol{E}\times\boldsymbol{B}}{B^2} + \frac{m{V_\perp}^2}{2qB^3}\boldsymbol{B}\times\boldsymbol{\nabla}(B) \\
&\quad + \frac{m{v_\parallel}^2}{qB^4}\boldsymbol{B}\times(\boldsymbol{B}\cdot\boldsymbol{\nabla})\,\boldsymbol{B} \\
&\quad + \frac{m}{qB^2}\boldsymbol{B}\times\frac{d}{dt}\left(\frac{\boldsymbol{E}\times\boldsymbol{B}}{B^2}\right) \\
\frac{dv_{gc,\parallel}}{dt} &= \boldsymbol{U}_E\cdot\left(\frac{\partial\boldsymbol{b}}{\partial t} + v_{gc,\parallel}\frac{\partial\boldsymbol{b}}{\partial s} + \boldsymbol{U}_E\cdot\boldsymbol{\nabla}\boldsymbol{b}\right) \\
&\quad \frac{q}{m}E_\parallel - \frac{\mu}{m}\frac{\partial B}{\partial s}
\end{aligned}
$$

Distribution of the magnetic field

- high β plasmoids produce a local deformation of the Chapman-Ferraro layer (*Heikkila, 1982*) and field line **interconnection** (*Lemaire and Roth, 1991*);
- a model magnetic field distribution of a TD is described by (*Lemaire and Burlaga, 1976; Roth et al., 1996*)

$$\boldsymbol{B}(x) = \frac{\boldsymbol{B}_1}{2} erfc\left(\frac{x}{L}\right) + \frac{\boldsymbol{B}_2}{2}\left[2 - erfc\left(\frac{x}{L}\right)\right]$$

Electric field for integration

- **CASE A**: uniform electric field

$$\boldsymbol{E}(x) = \boldsymbol{E}_A = \boldsymbol{cst} = -\boldsymbol{v}_{gc_1} \times \boldsymbol{B}_1 \qquad (2)$$

- **CASE B**: non-uniform, conserving U_E

$$\boldsymbol{E}_B(x) = -\boldsymbol{v}_{gc_1} \times \boldsymbol{B}(x) \qquad (3)$$

- **CASE C**: non-uniform, conserving $\overline{\mu^+} + \overline{\mu^-}$ (*Lemaire, 1985*)

$$\frac{d}{dt}\left(\frac{\boldsymbol{E}_c(x) \times \boldsymbol{B}(x)}{B^2}\right) + \frac{\overline{\mu^+} + \overline{\mu^-}}{m^+}\boldsymbol{\nabla}\left|\boldsymbol{B}(x)\right| \cong 0 \qquad (4)$$

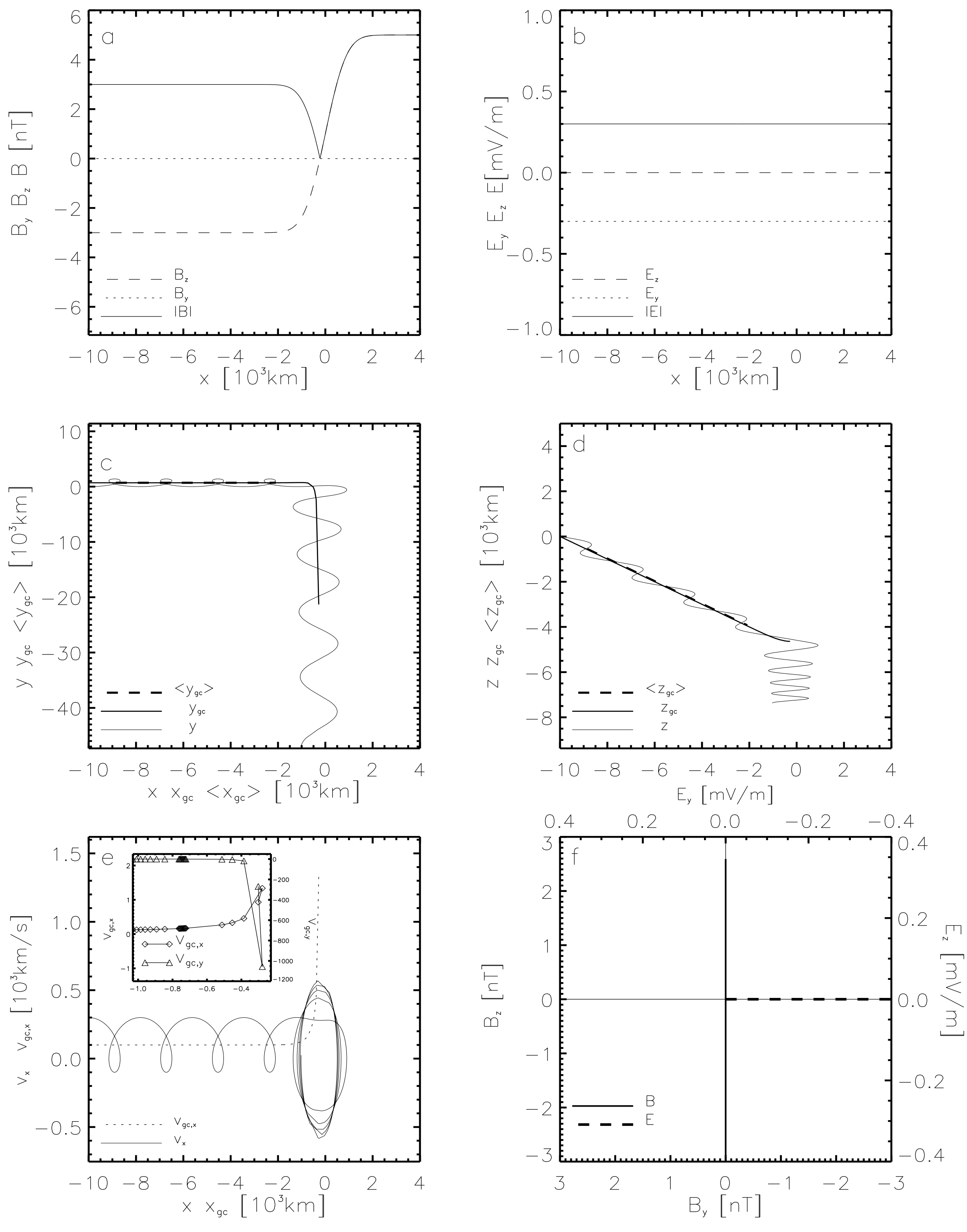

(electric field distribution of CASE A)

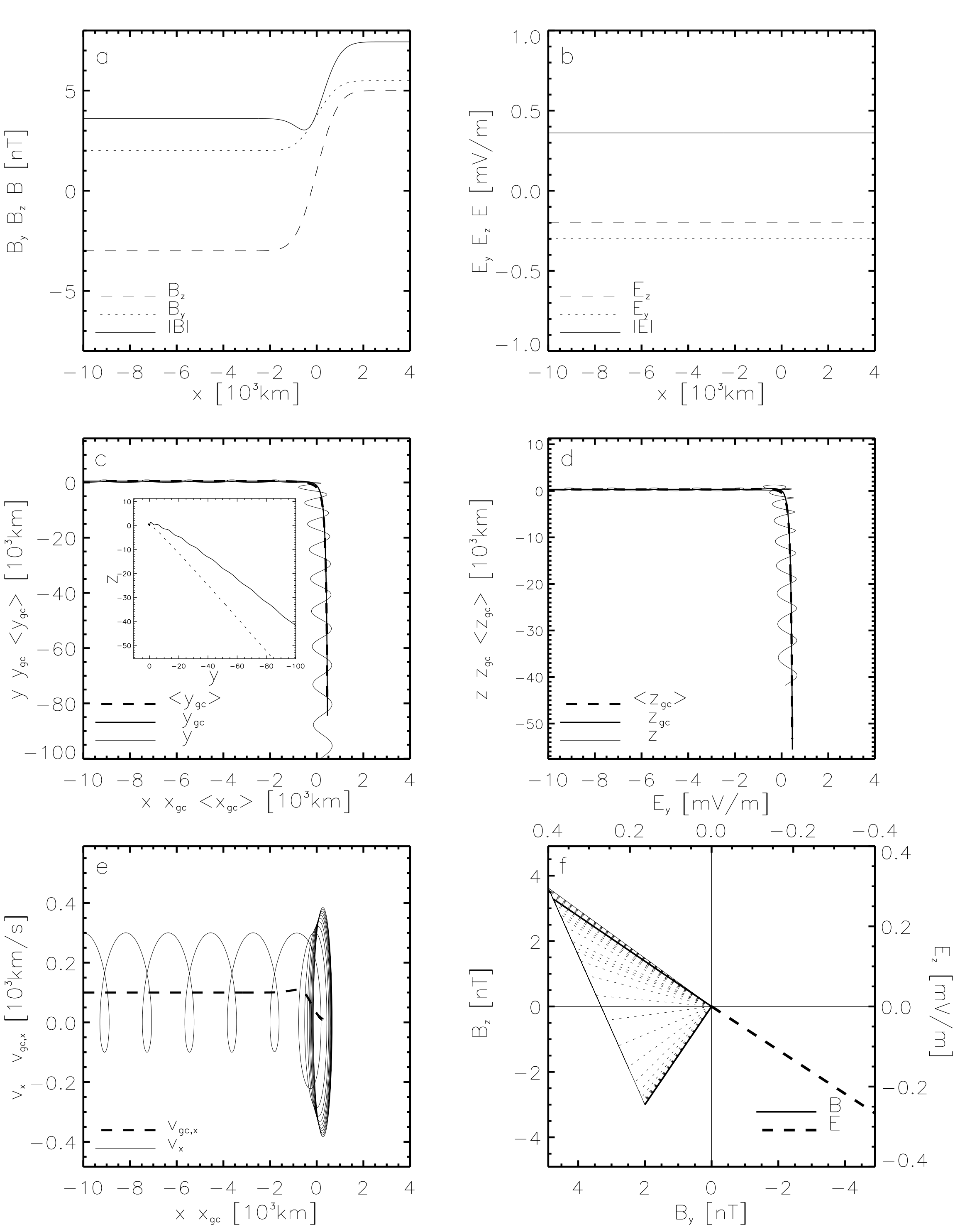

(electric field distribution of CASE A)

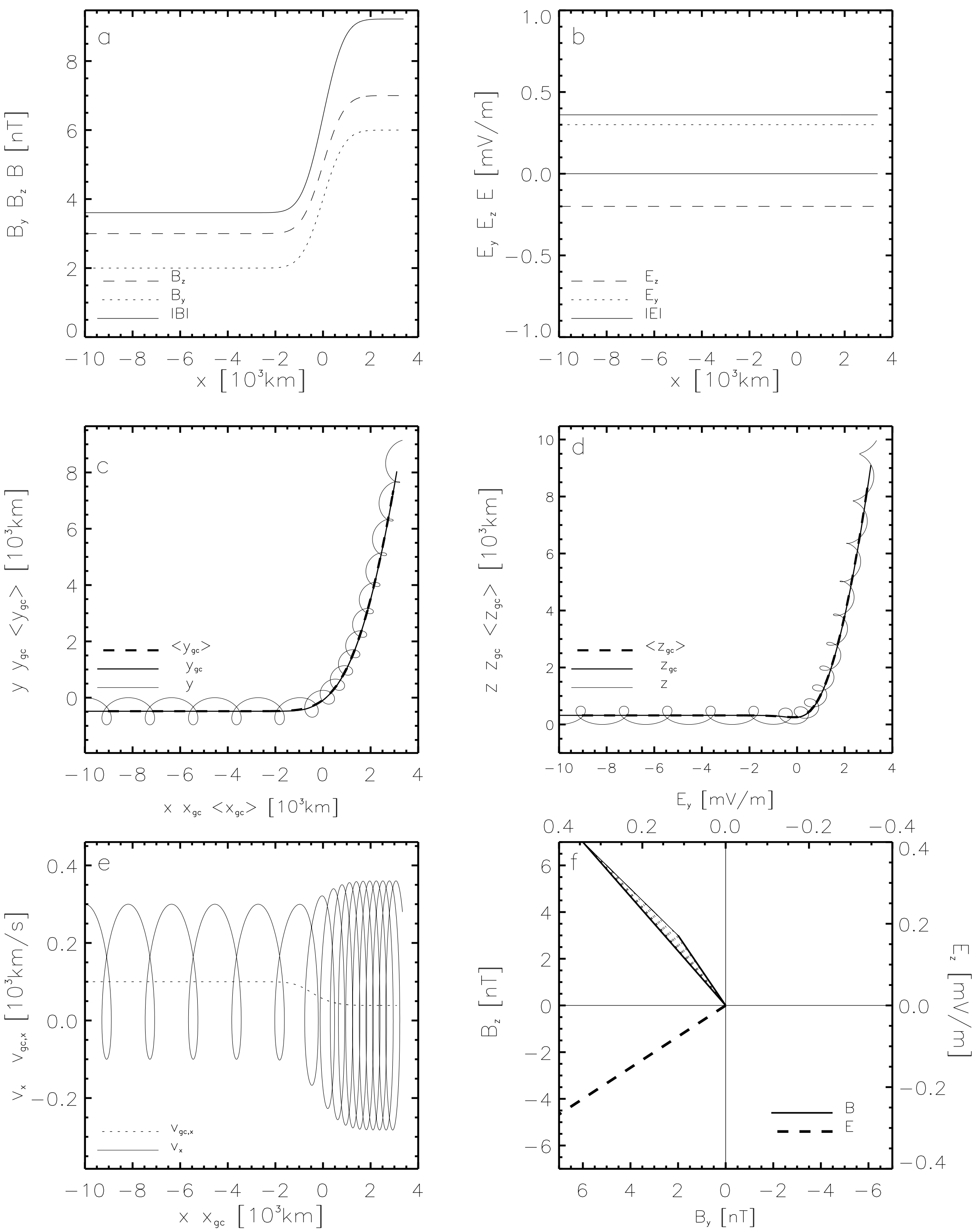

(electric field distribution of CASE A)

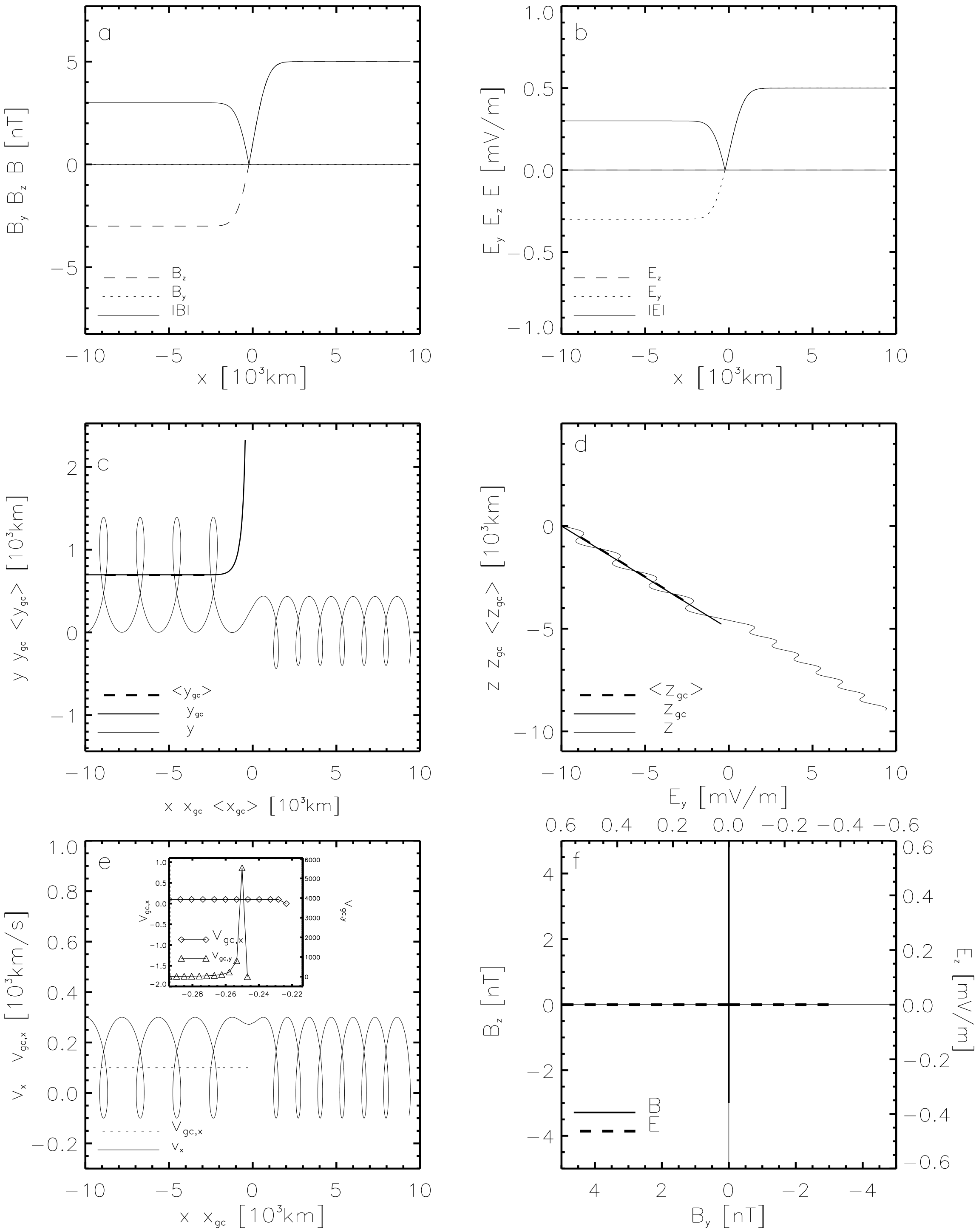

(electric field distribution of CASE B)

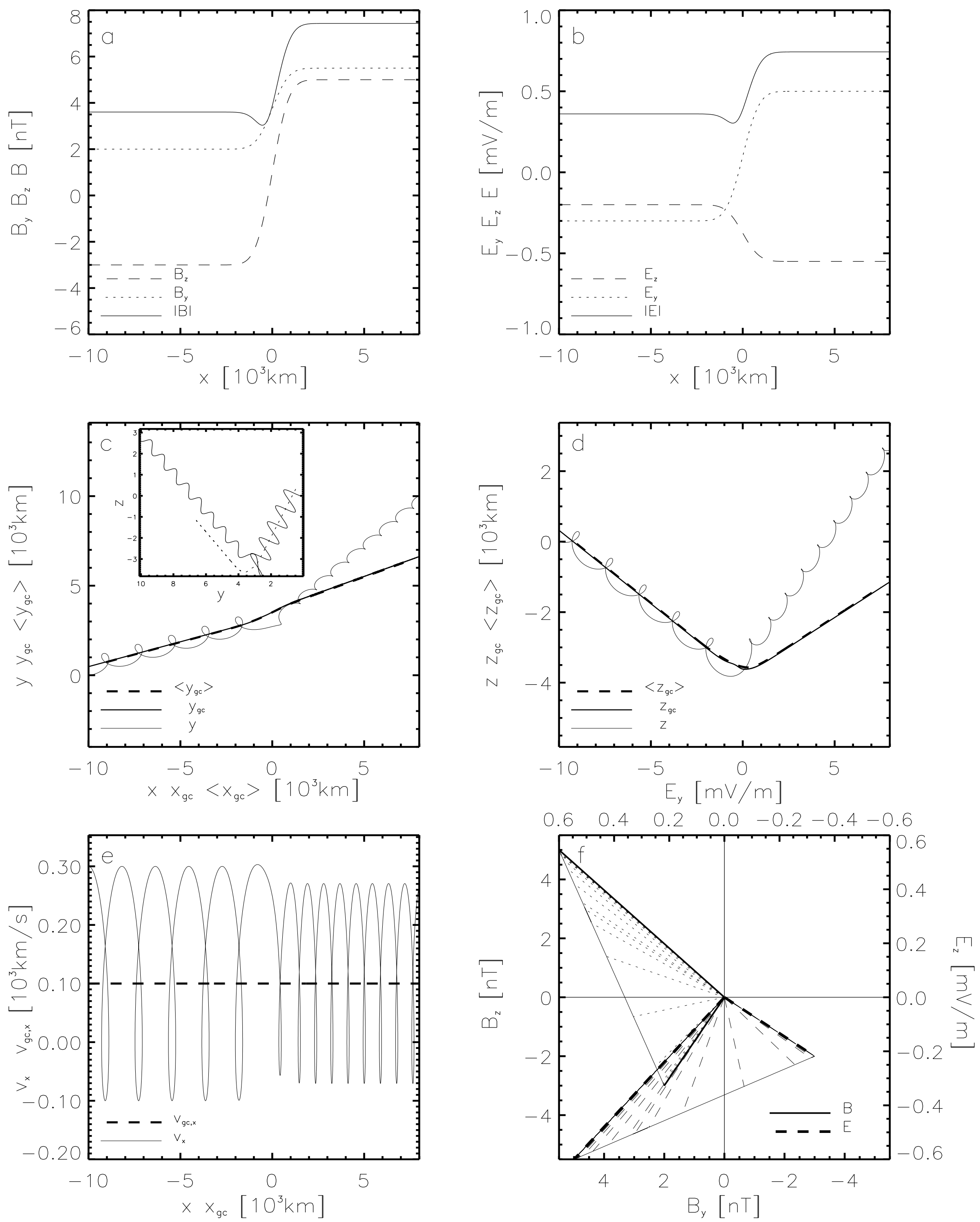

(electric field distribution of CASE B)

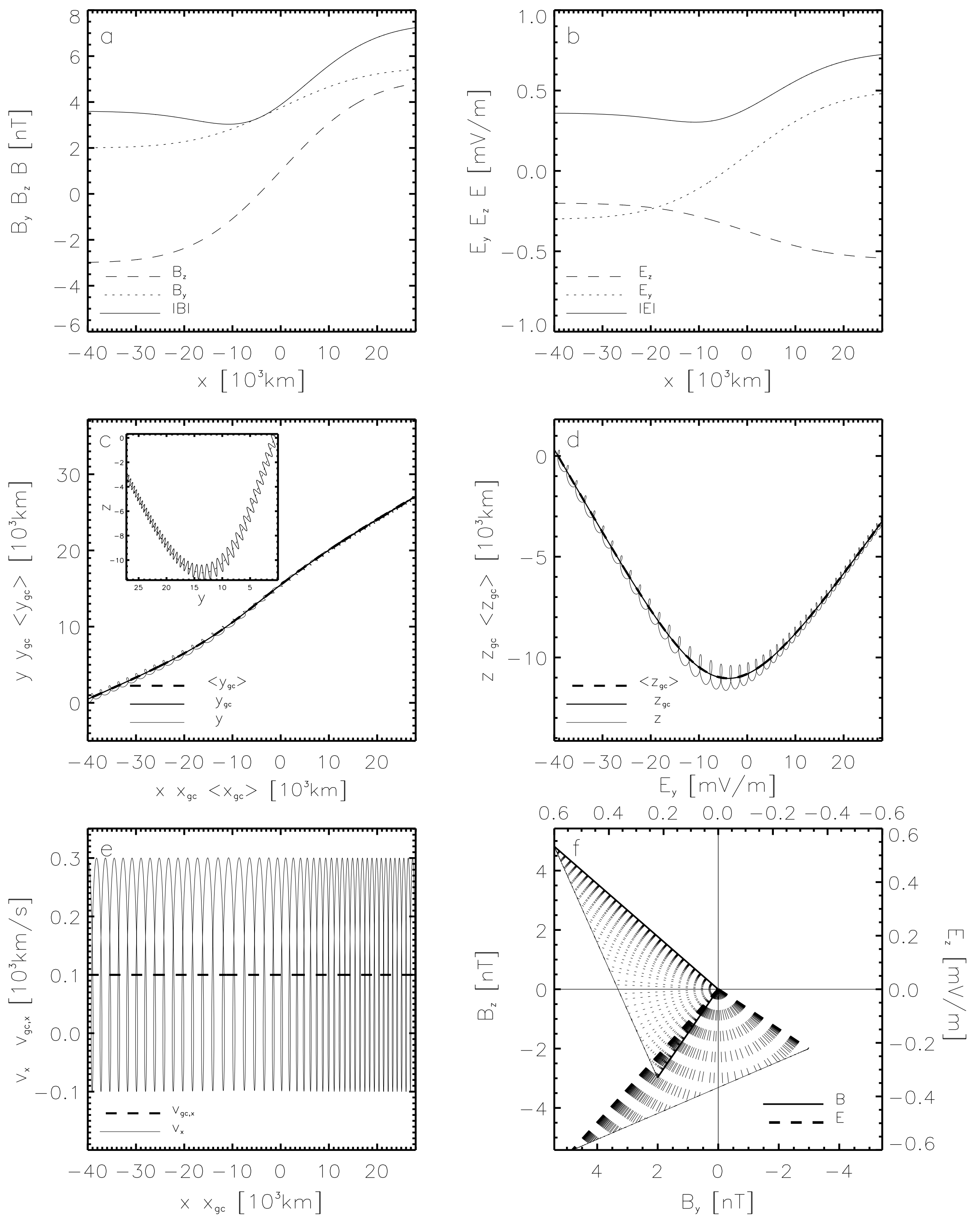

(electric field distribution of CASE B)

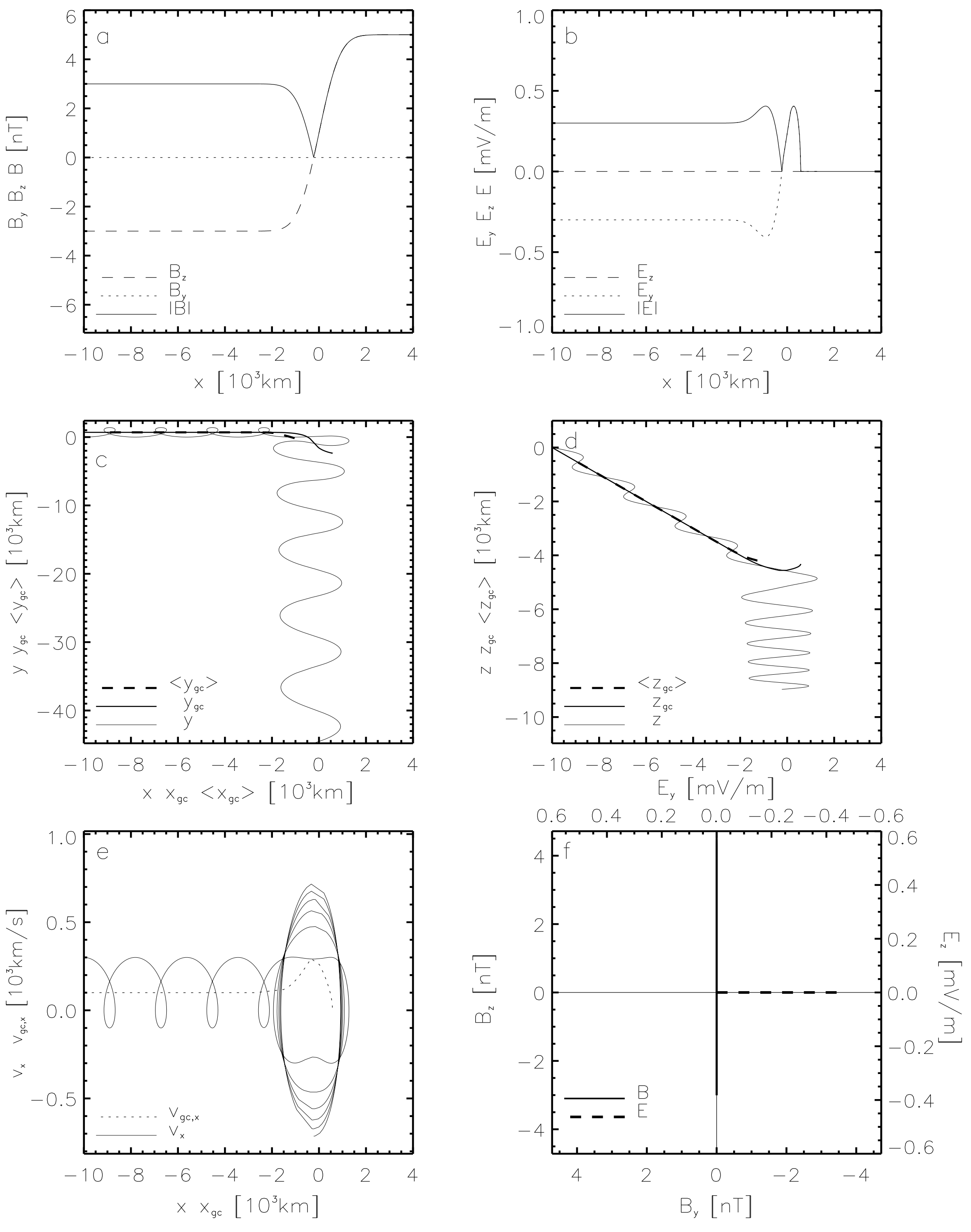

(electric field distribution of CASE C)

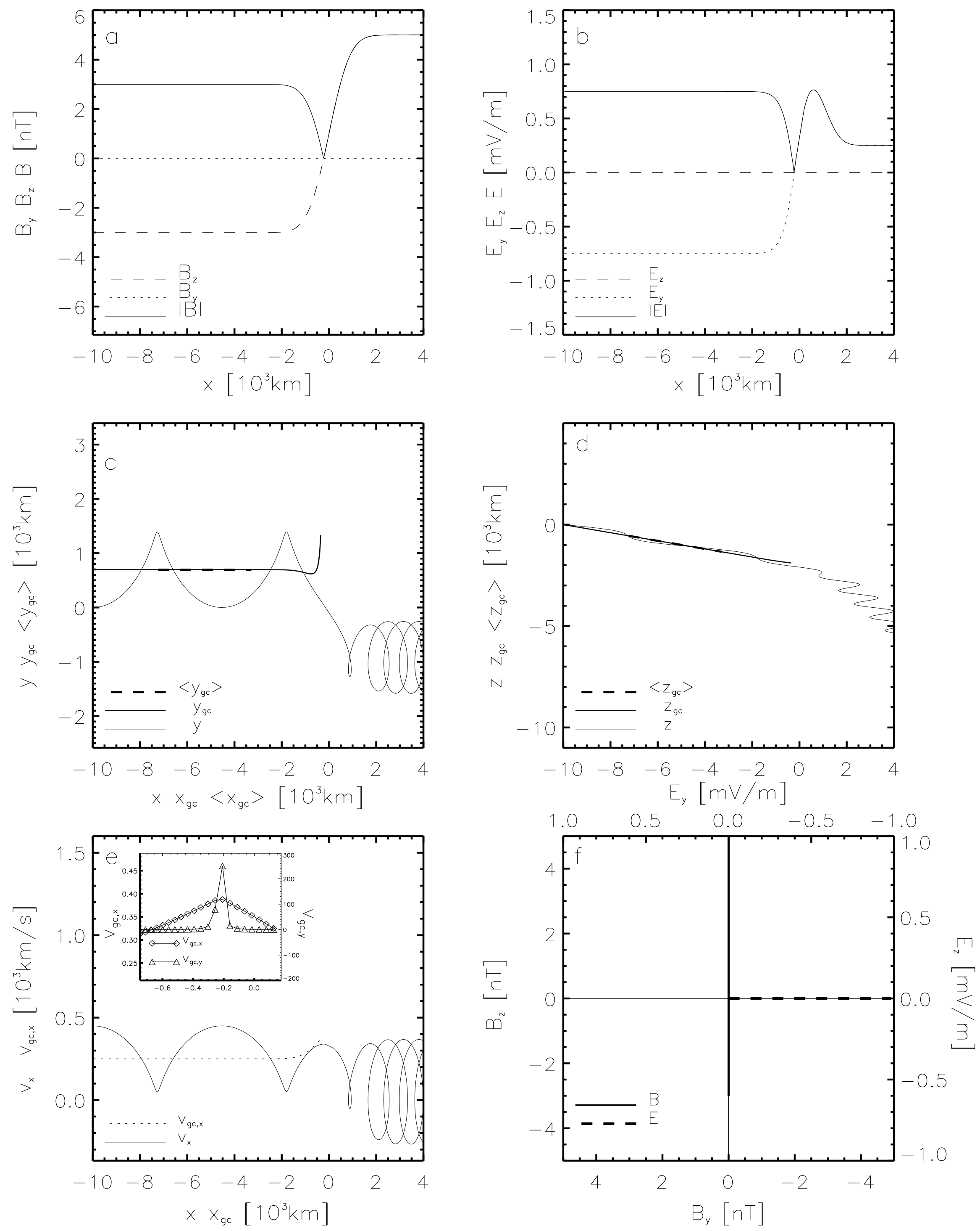

(electric field distribution of CASE C)

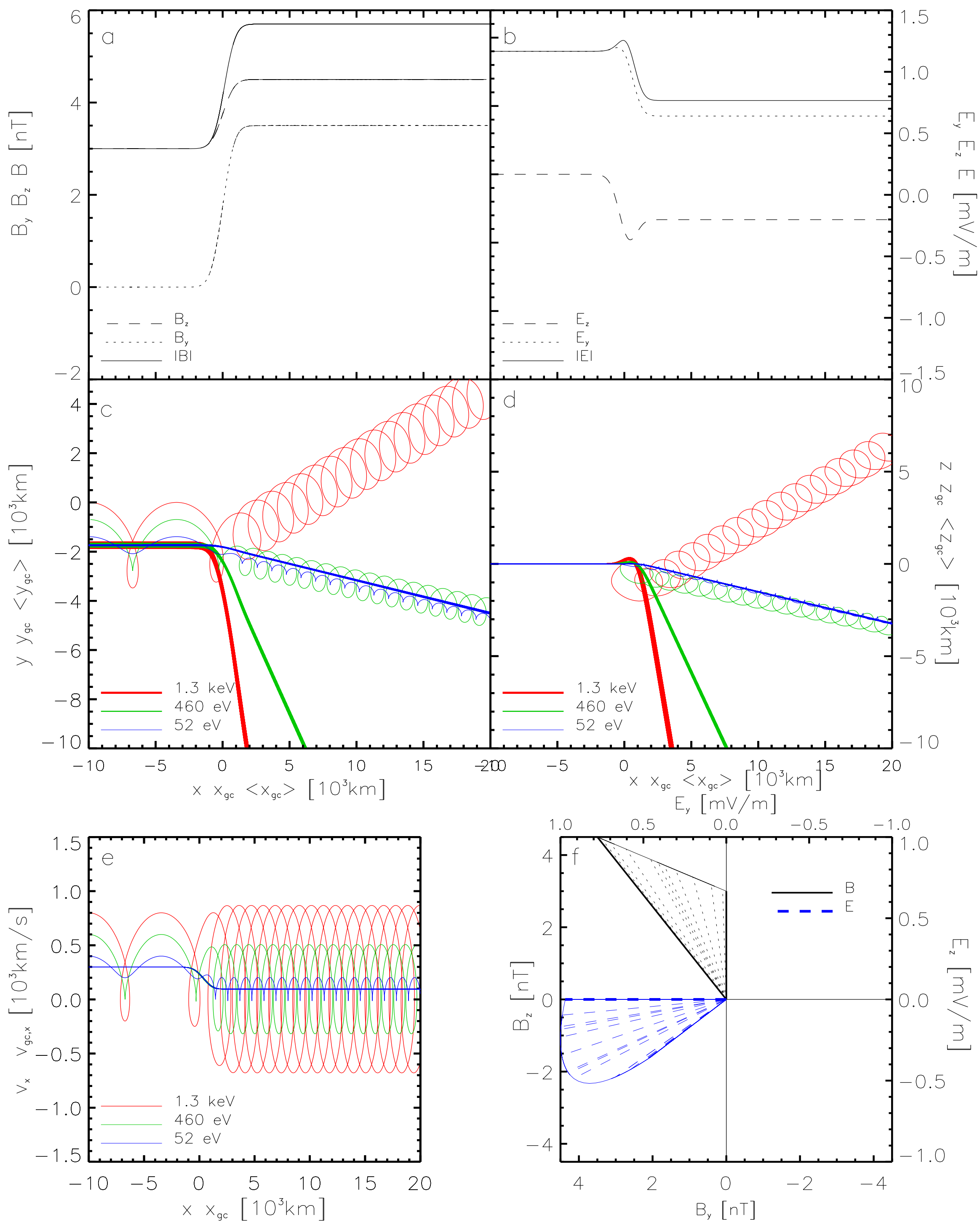

(electric field distribution of CASE C)

Conclusions

- electric field distributions, others than those of the early models of reconnection, have been successfully tested by numerical integration of single particle orbits
- the mathematical singular point of the first order approximation does not correspond to a "physical" singularity of the mechanical equation of motion of the particle
- numerical integration of orbits shows that ions and electrons can penetrate through the discontinuity
- nonadiabatic variations of $\boldsymbol{B}$ at the magnetopause invalidates the zero and first order (guiding center) approximations